frontiers | Frontiers in Earth Science

TYPE Original Research
PUBLISHED 08 March 2023
DOI 10.3389/feart.2023.1023773

OPEN ACCESS

EDITED BY
Liangren Zhang,
Nanjing University, China

REVIEWED BY
Karoly Nemeth,
Institute of Earth Physics and Space Sciences, Hungary
Junna Zhang,
Beijing Normal University, China

*CORRESPONDENCE
Huiru Lian,
huiru@ustb.edu.cn

†These authors have contributed equally to this work and share first authorship

SPECIALTY SECTION
This article was submitted to Quaternary Science, Geomorphology and Paleoenvironment, a section of the journal Frontiers in Earth Science

RECEIVED 20 August 2022
ACCEPTED 20 February 2023
PUBLISHED 08 March 2023

CITATION
Lian H, Xu T, An W, Zhu Y, Shi H, Zhao Y and Chen K (2023), Site formation process of the Dadong Paleolithic site in Jilin province, China: A geoarchaeological approach. *Front. Earth Sci.* 11:1023773. doi: 10.3389/feart.2023.1023773

Site formation process of the Dadong Paleolithic site in Jilin province, China: A geoarchaeological approach

Huiru Lian[1]*†, Ting Xu[2†], Wenrong An[3], Yujin Zhu[4], Hongwei Shi[4], Ying Zhao[5] and Kunlong Chen[1]

[1]Institute for Cultural Heritage and History of Science and Technology, University of Science and Technology Beijing, Beijing, China, [2]Zhejiang University City College, Hangzhou, China, [3]Jilin Provincial Institute of Cultural Relics and Archaeology, Changchun, China, [4]School of Geography, Nanjing Normal University, Nanjing, China, [5]Jilin Confucian Temple Museum, Jilin, China

The Dadong site, located in the Changbaishan region of Jilin province, China, is an important Upper Paleolithic site characterized by its large distribution area and abundant stone artifacts. This study presents a geoarchaeological study of a newly excavated area of this site. Soil micromorphology, particle size analysis, and pH measurements were used to reconstruct the site formation process from around 60 ka to the present. Additionally, this study examines the impact of volcanic eruptions and local geomorphology on ancient human adaptation in this area. This paper also investigates the effects of post-depositional processes, particularly freeze-thaw, on the distribution of lithics. This study is the first soil micromorphological study of a Paleolithic site in Northeast China, and is important for studying the changes of the Pleistocene environment in this region as well as the development of microblade technology in Northeast Asia.

KEYWORDS

site formation process, soil micromorphology, upper paleolithic site, postdepositional process, North-east Asia, Geoarchaeology

1 Introduction

Microblade technology, characterized by pressure knapping, various types of wedge-shaped micro-cores, and transverse burins with marginal retouch, is one of the most noteworthy phenomena in the Upper Paleolithic of northern Eurasia (Keates et al., 2019; Yue et al., 2021; Kato, 2022). Since its appearance around 28 ka cal BP, this technology has spread extensively throughout Northeast China, the Korean Peninsula, the Japanese Archipelago, the Russian Far East, and North America (G´omez Coutouly, 2018; Kato, 2022). However, there is a heated debate regarding the geographical and chronological origin of this technology. Different interpretations of site chronology and varying understandings of the microblade technology have led to diverse theories about the origin of this technology, with potential locations including southern Siberia, the Korean Peninsula, Northeast China, and the Hokkaido Island of Japan (Derevianko et al., 1998; Graf, 2009; Kato, 2022; Kuzmin and Keates, 2021; Yi et al., 2016; Yue et al., 2021 etc.).

Northeast China is a crucial region for comprehending the spread of microblade technology and the underlying population movements and cultural interactions. One the one hand, it is situated in a vital geographic position that connects the continental Asia, peninsular Korea, the Russian Far East, and beyond to the Japanese archipelago (Yue et al.,

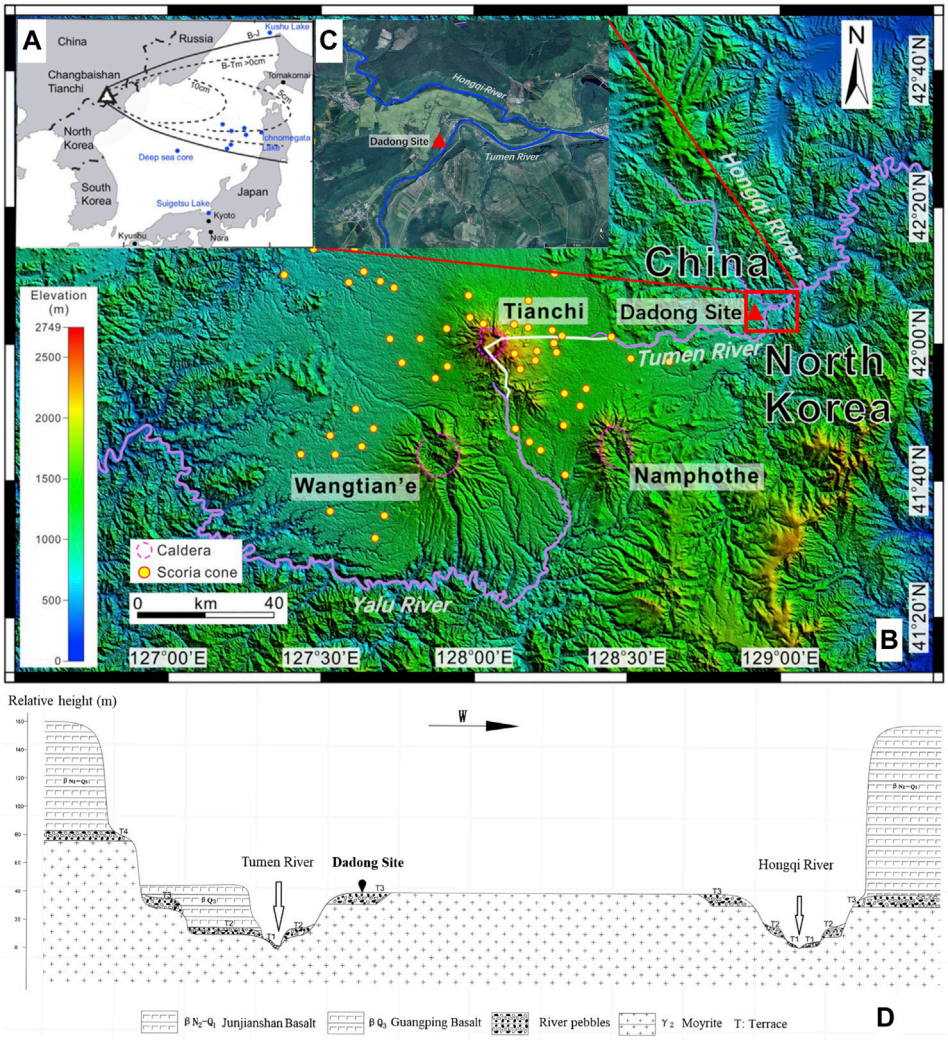

FIGURE 1
Geographic map around the Dadong site: **(A)** The location of Tianchi volcano and the extents of ashfalls of Baegdusan-Tomakomai tephra (B-Tm) and Baegdusan-Japan Sea tephra (B-J), photo adapted from Pan et al., 2020; **(B)** DEM map showing distribution of polygenetic volcanoes and representative monogenetic volcanoes around the Dadong site. The thick solid white line and the Tumen and Yulu Rivers are the border between China and North Korea. Photo modified from Zhang et al., 2018; **(C)** Enlarged map showing the detailed location of the Dadong Site (modified from Google Maps); **(D)** Schematic diagram showing the geomorphology of the Dadong site.

2021; Figure 1A). On the other hand, important Upper Paleolithic sites containing early blade and microblade assemblages, such as the Xishantou and Dadong sites, have been discovered in this region (Zhao et al., 2016; Wan et al., 2017; Liu et al., 2019). Among the Northeast China, the Changbaishan (also named Paektusan or Baekdusan) region is unique as it is under the direct influence of the Changbaishan volcanoes, a long-lived volcanic cluster active throughout the Pleistocene and Holocene (Zhang et al., 2018; Pan et al., 2020). Volcanic activities form special landform, provide both risks and resources for Paleolithic human occupation. One of the most important resources is obsidian, a high-quality raw material that is considered closely related to the emergence of pressure flaking technique in Korea (Lee and Kim, 2015; Kuzmin, 2019). In recent years, hundreds of Upper Paleolithic sites have been discovered near the Changbaishan volcanoes. The majority of these sites were open-air, located on river terraces such as the middle and upper reaches of the Tumen River and the upper reaches of the Songhua River (Guo, 2021; Xu et al., 2021). Abundant obsidian stone artifacts produced by both blade and microblade technology were unearthed (Chen and Wang, 2008). For these open-air sites, it is vital to investigate whether artifacts were found within sediments as transported clasts, or were *in situ* materials. What mode of deposition dominated the deposition process and the degree of post-deposition disruption on artifacts are also important issues needed to be addressed (Macphail and Goldberg, 2017). However, little research has been conducted on the site integrity, formation process, paleoenvironment, and the impact of volcanism on human adaptation to these sites. As a result, the discussion of microblade technology in this significant region, as well as an accurate understanding of the lithic assemblages and site chronology, has been constrained (G´omez Coutouly, 2018).

Micromorphological methods, together with sedimentological and other geoarchaeological techniques, have been widely and successfully applied in various open-air Paleolithic sites across the world to reconstruct the formation process (e.g., Mallol, 2006; Boness and Goren, 2016; Krajcarz et al., 2016; Glauberman et al., 2020) and to identify the characteristics and evolution of the local landscape, resources, climate, and vegetation of the surrounding area (e.g., Marder et al., 2011; Sedov et al., 2011; Stahlschmidt et al., 2018). However, in China, the application of micromorphological methods in Paleolithic sites remain scarce. The most well-known micromorphological research in China is the study of the 'hearth' in Zhoukoudian Locality 1, which was first believed to have early evidence of fire (Jia and Huang, 1984) but was later questioned by micromorphological research (Weiner et al., 1998; Goldberg et al., 2001). Other important Paleolithic cave sites in China, such as Xianrendong (Patania et al., 2019) and Yuchanyan (Patania et al., 2020), have also involved micromorphological studies to examine the site formation processes, stratigraphic integrity, and spatial use of the site. The application of micromorphological methods in open-air sites is also limited, except for the research conducted by Jin and Guo. (2011), Song et al. (2017) and Li et al. (2021). Their studies provided stratigraphic and environmental data for a systematic interpretation of human use of the site, as well as a reconstruction of the site's sedimentary process.

This study proposed to use soil micromorphology, particle size analysis, and pH measurements to study a representative and well-excavated Upper Paleolithic site, the Dadong site in South Changbaishan region, Jilin province, China. The results of this study shed light on the formation process and the effects of volcanic eruptions and local geomorphology on human activities of this important site, which is vital for understanding human adaptation, migration, as well as microblade technology development in this key area of Upper Paleolithic human occupation. This research also serves as a valuable analogue for studying other Upper Paleolithic sites in the region, and may promote the application of micromorphological methods in China.

2 Materials and methods

2.1 The Dadong site

2.1.1 Regional setting and background

The Dadong Upper Paleolithic site (N 42°05′37.9″, E128°57′30.2″) is located in the northeast of the Dadong Village in Helong City, Jilin Province, China (Figure 1B). This site is around 75 km west of the Changbaishan volcanoes, and volcanic activity has played a key role in shaping the geological features of this region.

Changbaishan volcanoes are intraplate stratovolcanoes located on the border between China and North Korea (Sun et al., 2018). This volcanic group has undergone three major evolutionary stages: (1) a basaltic shield-forming stage lasting from the Pilocene to the early Pleistocene; (2) a basaltic to trachytic composite cone-forming stage in the Pleistocene, which forms three main polygenetic cones (i.e., Namphothe volcano in North Korea, Wangtian'e volcano in China, and Tianchi volcano straddling both countries) and hundreds of monogenetic scoria cones; and 3) an explosive stage, with eruptions of comendite (rhyolite) and trachyte magma (Wei et al., 2013; Zhang et al., 2018; Pan et al., 2020).

While the Wangtian'e and Namphothe volcanoes stop being active since 2 Ma and 1 Ma, respectively, the Tianchi volcano has been active throughout the Late Pleistocene and Holocene (Liu et al., 2015). The time boundary between the second stage (effusive eruptions producing voluminous basaltic magmas) and third stage (explosive eruptions producing substantial pyroclastics) of the Tianchi volcano is unclear now (Zhang et al., 2018). However, distal Tianchi-sourced tephra deposits from the Japan Sea (Figure 1A) suggest that Plinian-type eruptions of Tianchi volcano occurred in the Late Pleistocene, with one of the largest volume explosive events (VEI7), Baegdusan-Japan Sea tephra (B-J), being dated to 50.6 ka (Okuno et al., 2011; Lim et al., 2013; Pan et al., 2020). After a hiatus of almost 43 ka, the Tianchi volcano was erupted again at 8–4 ka (Qixiangzhan event), 946 CE (the Millennium Eruption with a VEI≥7, B-Tm tephra in Figure 1A), 1403 CE, 1668 CE, 1702CE, and 1903 CE (Wei et al., 2013; Sun et al., 2018; Pan et al., 2020). In addition, Strombolian-type eruptions of monogenetic volcanoes extensively scattered around the Tianchi volcano and small-scale fissure eruptions also took place during the post-shield stage (1.17–0.05 Ma) (Zhang et al., 2018).

The Tumen River rises in the east flank of the Tianchi volcano and partition China from North Korea (Figure 1B). On the east side of the upper Tumen River, four terraces have formed. Terraces 3 and 4 are commonly covered with Junjianshan Basalt and Guangping Basalt that formed between 5.5 and 0.19 Ma (Figure 1C). On the west side, three terraces are exposed. The T3 terrace is approximately 40 m above the current river surface and is wide and flat. Mesozoic moyite forms the foundation of this terrace (Fan et al., 2006), which is later covered by basaltic fluvial gravels and albic soils. The Dadong site is situated on this T3 terrace (Figure 1C). To the west of the Dadong site, the Hongqi River (a tributary of the Tumen River) has downcut this flat-table shaped terrace, forming three terraces as well, making the T3 terrace relatively isolated.

A temperate continental monsoon climate prevails in the South Changbaishan region, resulting in four distinct seasons. The annual precipitation is 573.6 mm. The annual average temperature is 5.6°C, with extreme maximum and minimum temperatures of 36.2°C and −31.5°C, respectively. Temperate coniferous and broad-leaved mixed forest dominate the vegetation (Chang et al., 2018). High-resolution lake and peat sedimentary sequences near Changbaishan record the history of climate and vegetation changes in the Late Pleistocene: the transition into the Last Glacial Maximum (LGM) in this region began at ca. 29.5 cal kyr B.P.; after the LGM (25.6–18.2 cal kyr B.P.), two cold events occurred at ca. 17.6–14.5 cal kyr B.P. and ca. 12.7–11.7 cal kyr B.P (Younger Dryas event) (Stebich et al., 2009; Ge, 2012; Mingram et al., 2018).

2.1.2 Site information and stratigraphy sequence

The Dadong site was discovered and excavated in 2007, and was further excavated in 2010 and 2021 (Li, 2008; Zhao, 2012; Li et al., 2016; Wan et al., 2017). The current investigation reveals that the Dadong site covers an area of around four square kilometers. In all excavation areas of the Dadong site, the general sequence consists of seven major layers from top to bottom. The first layer (5–10 cm thick) is loose, yellowish-brown topsoil rich in humus. The second layer (2–5 cm thick) is grayish-white volcanic ash, which was not

FIGURE 2
Stone artifacts from the Dadong site: 1. Stone hammer, Layer 5; 2. End scrapper, Layer 5; 3. Blade core, Layer 4; 4. Burin, Layer 5; 5. Core, Layer 4; 6. Point, Layer 3; 7. Wedge-shaped microcore, Layer 3; 8. Single-platform core, Layer 3; 9. Photo of Layers 1-6, note the vertical ice wedges filled with grayish-white sediment in the upper part of the profile. The circular scale has a diameter of 5 cm; 10. Details of Layer 7, note the mixture of gravels and coarse sands.

well exposed in the 2021 excavation area. The third, fourth, and fifth layers are compact, blocky silty clay with different soil colors ranging from grayish-brown (20–30 cm thick), black (40 cm thick), and yellow (30 cm thick). Ice wedges were found in Layer 3 and penetrated Layers 4 and 5 (Figure 2). These three layers yielded abundant stone artifacts. The sixth layer (120 cm thick) is composed of loose, yellowish-brown silt. Two sub-layers, 6A and 6B are further subdivided based on the change of grain size. Layer 7 at the bottom is basaltic gravels mixed with coarse sands (Figure 2).

Stone artifacts were primarily discovered in Layers 1, 3, 4, and 5. In field season 2007, 5681 stone artifacts were recovered (Wan et al., 2017); in field season 2021, over 8000 stone artifacts were recovered. Lithic artifacts constitute the exclusive cultural remains at the site. Stone implements recovered from these seasons are all dominated by high quality obsidians, which are regarded as a high-quality raw material suitable for pressure flaking (Yue et al., 2021), and included the types of cores, flakes, blades, microblades, chunks and tools (Li, 2008; Wan et al., 2017). Previous research suggests that scrapers, burins, points, notches, backed knives, boring tools and arrowheads constituted the tool assemblage, which are mostly made from blades through elaborate retouch (Zhao, 2012; Wan et al., 2017). Detailed excavation in 2021 further ascertained that Layers 1 and 3 exhibit similar traits that wedge-shaped microblade core technology based on bifacial blank was observed. Layers 4 and 5 are similar in that only blade technology and tools such as burins and scrapers are found (Figure 2). A few stone artifacts were also discovered in Layer 6 but are relatively small sized.

Previous radiocarbon dating shows that the Layer 4 from the 2010 excavation is dated to 25900–25340 cal kyr B.P. (Zhao et al., 2016; Wan et al., 2017). Recent OSL and radiocarbon dating of the 2021 profile suggests that Layer 3 was dated to approximately 15 ka, Layer 4 to around 25 ka, and Layer 5 to around 27 ka. Layers 6 and 7 were deposited between 60 and 40 ka. A detailed chronology of the Dadong site will be published separately.

2.2 Methods

2.2.1 Sampling strategy

The sediment and soil samples were collected from Trench TG1, which is located north of the 2021 excavation area (Profile

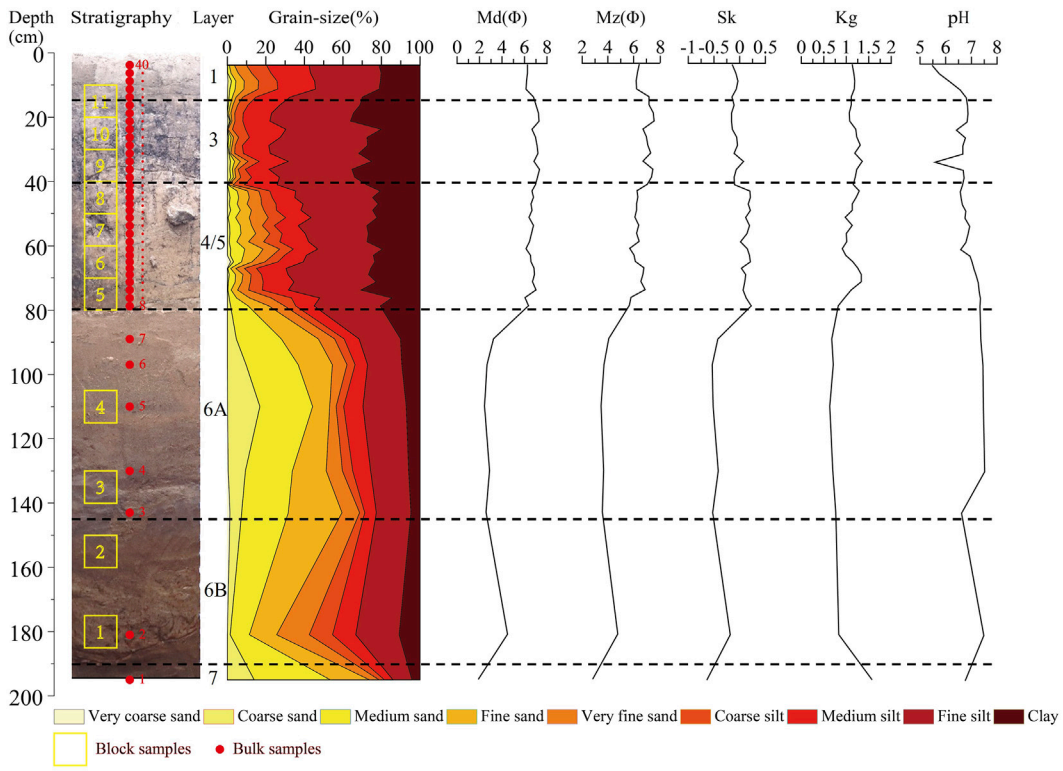

FIGURE 3
Stratigraphy of the Dadong Site and the soil sampling positions (left); analytical results of particle size analysis and pH measurement (right).

JHDDTG1) and around 20 m west of the Tumen River. Micromorphology samples 10 cm × 10 cm × 10 cm in size were taken continuously from 10cm to 80 cm from the surface, corresponding to Layers 1, 2, 3, 4, and 5 of the Dadong site's standard stratigraphy. Subsequently, samples were taken selectively at 105–115 cm, 130–140 cm, 150–160 cm and 175–185 cm from the surface (Figure 3). They correspond to Layer 6 of the standard stratigraphy. Bulk samples were taken adjacent to the micromorphology samples for particle size and pH analyses. Around 150 g bulk samples were taken at 2.5 cm intervals from 5 cm to 80 cm from the surface, corresponding to Layers 1, 2, 3, 4, and 5 of the Dadong standard stratigraphy. Subsequently, samples were taken at 88–90 cm, 96–98 cm, 109–111 cm, 129–131 cm, 142–144 cm, 180–182 cm, and 194–196 cm from the surface, corresponding to Layers 6 and 7 of the standard stratigraphy (Figure 3). In total, 40 bulk samples and 11 intact soil and sediment blocks were collected for laboratory analyses.

2.2.2 Analytical methods

Soil micromorphology, the study of undisturbed samples of soil, sediment, and archaeological materials at the microscopic level (Courty et al., 1989), is a useful technique to reveal detailed and subtle changes in the environment and sedimentation as well as anthropogenic features (French, 2003, chapter 4; Goldberg and Macphail, 2006, chapter 16). The micromorphology slides were prepared at a commercial laboratory (Jiuren Kuangye) in Beijing, described with a Leica DM2700 polarizing microscope, and photographed with a Langyan VTX20 digital camera and software system at the University of Science and Technology Beijing. The description of the thin sections follows the descriptive system developed by Bullock et al. (1985) and Stoops (2003).

Particle size analysis, the study of the sizes and distributions of sediments under investigation, has long been used to detect the source, hydrodynamic conditions, and sedimentation processes, and can therefore provide a larger regional environmental context for archaeological sites (Boggs, 2001; Catt, 1985; Goldberg and Macphail, 2006, chapter 16). The analysis of pH provides a basic soil and sediment environment background for the results of other bulk analysis methods (Goldberg and Macphail, 2006, chapter 16). These sets of information could be both complementary to and corroborated by features and observations obtained from the micromorphological analysis, and combined to suggest the changing nature of past environments as well as human impact and post-depositional processes (Macphail and Goldberg, 2017).

The particle size analysis and pH measurement were conducted at the School of Geography of Nanjing Normal University. Prior to measurement, organic matter and calcium carbonate were removed with the successive addition

10.3389/feart.2023.1023773

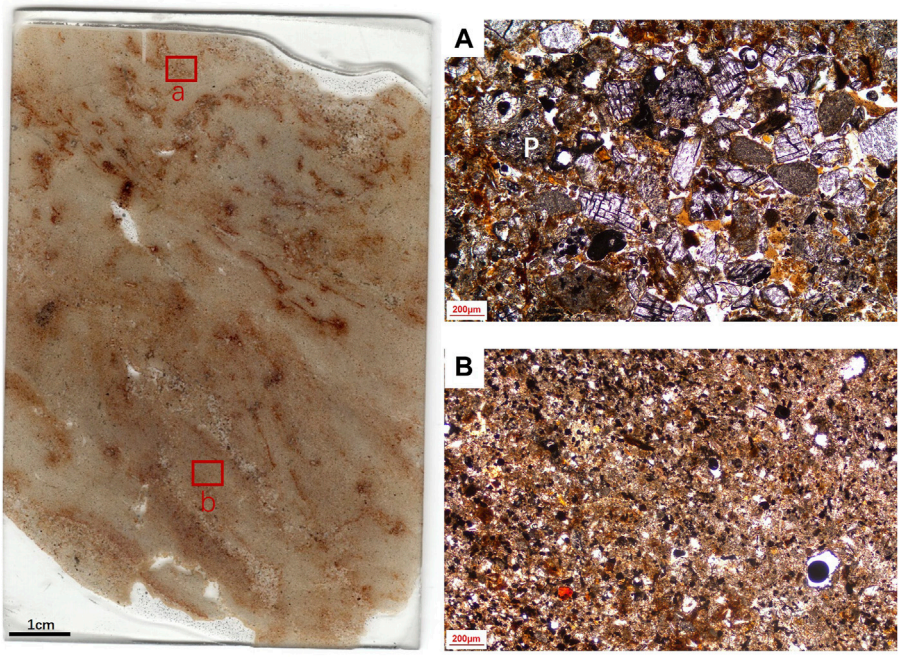

FIGURE 4
Scan of the thin section from block sample DD1. Abundant reddish-brown sesquioxide can be seen. **(A)** infillings of well-sorted fluvial sands (PPL), P: pumice. **(B)** fine silty clay groundmass (PPL).

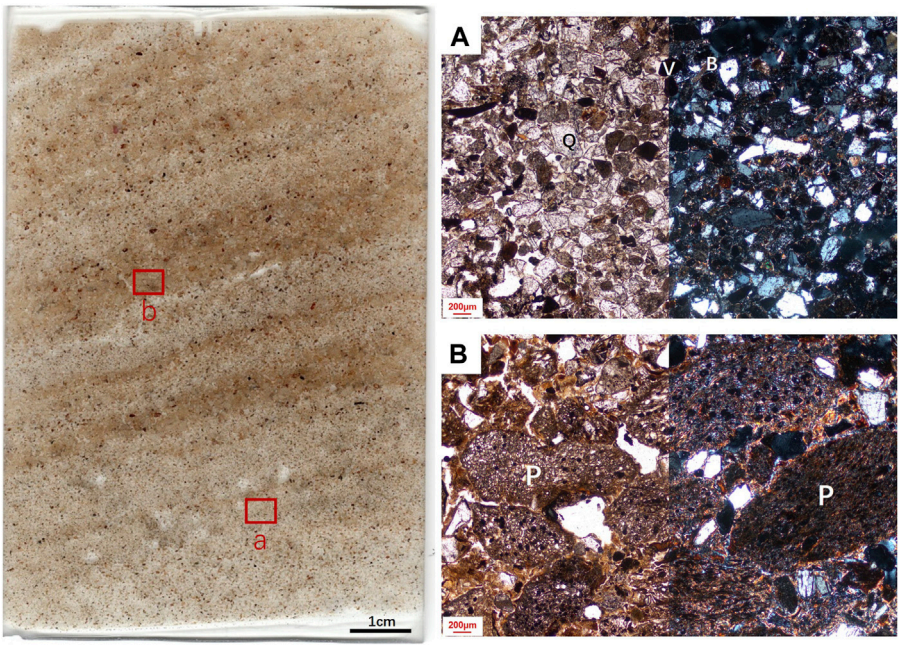

FIGURE 5
Scan of the thin section from block sample DD4. Alternations of dark brown tephra layers and light brown fluvial sands can be seen. **(A)** fine to medium sand size, sub-rounded fluvial sands; widely found volcanic glass show igneous lithologies (PPL and XPL), V: volcanic glass; B: bitotite; Q: quartz. **(B)** tephra layer, with a pellicular to intergrain micro-aggregate structure (PPL and XPL), P: pumice.

10.3389/feart.2023.1023773

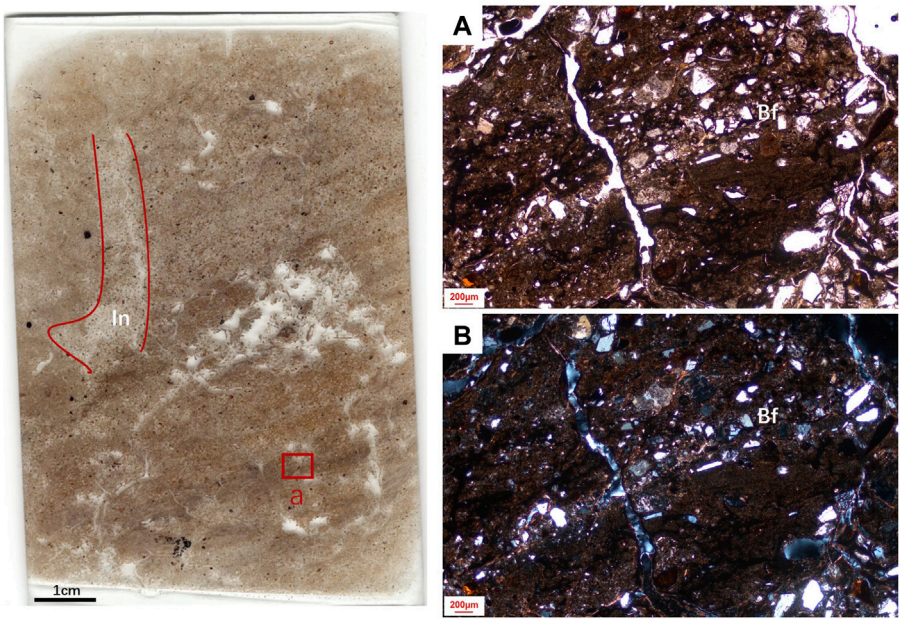

FIGURE 6
Scan of the thin section from block sample DD7; the upper fabric is mainly composed of fluvial sands, vertical long cracks later filled by coarse silt and fine sand (In) are marked by red lines; the lower fabric is finer and darker. **(A)** and **(B)**: banded fabrics related to alternating freeze and thaw (PPL and XPL), Bf: banded fabric.

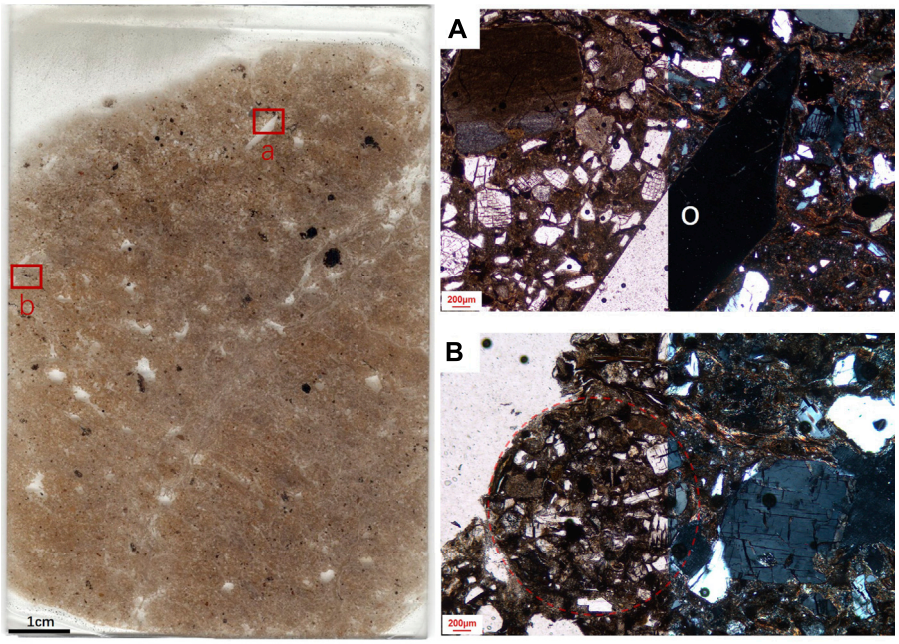

FIGURE 7
Scan of the thin section from block sample DD9. **(A)** obsidian stone artifact, vertically aligned (PPL and XPL), O: obsidian; **(B)** granular aggregates (PPL and XPL), marked by red lines.

of hydrogen peroxide and hydrochloric acid. The Mastersizer 3000 laser particle sizer was used to measure the prepared samples. A calibrated METTLER TOLEDO SevenCompact Bench pH meter was used to test the pH value. Each sample was tested three times, and the average value was taken as the final result.

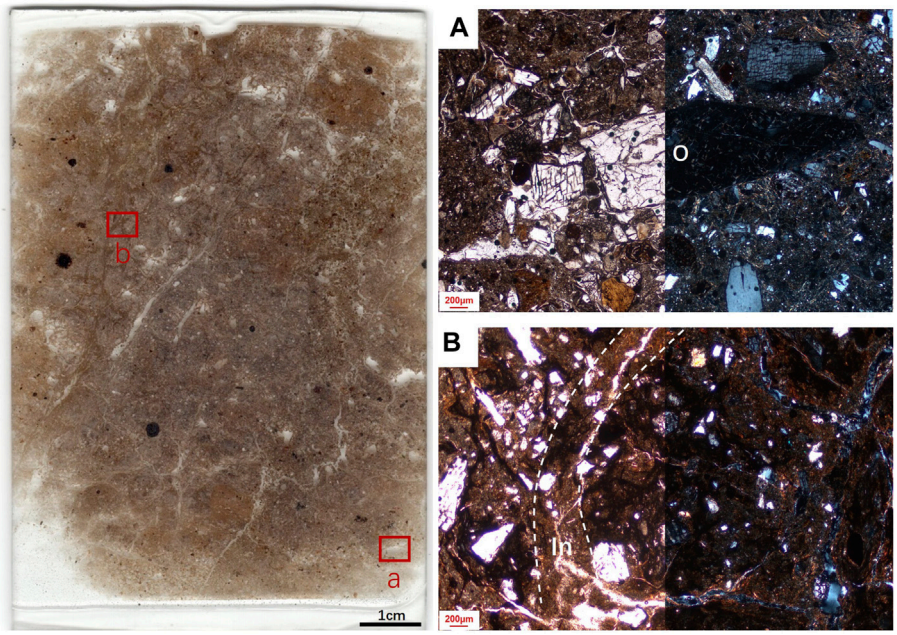

FIGURE 8
Scan of the thin section from block sample DD10. **(A)** obsidian stone artefact (PPL and XPL), O: obsidian. **(B)** fine-grained material infilled the voids between granular aggregates (PPL and XPL), the infilled area (In) is marked by white lines.

3 Results

3.1 Soil micromorphology analysis

The stratigraphy observed under the microscope agrees with the general sequence established in the field, which consists of seven major layers. Here we present the interpretative description of the micromorphological samples. A detailed description of each micromorphological sample can be found in Supplementary 1. The main micromorphological properties of Trench TG1 are illustrated in Figure 4; Figure 5; Figure 6; Figure 7; Figure 8.

3.1.1 Layer 6B

Layer 6B (Samples DD1 and DD2) shows a massive microstructure, with 5% voids. The groundmass is dominated by fine silty clay and moderately sorted, fine sand-sized quartz grains ($c/f_{50\mu m}$: 40: 60), with a speckled b-fabric (Figure 4B). There are a few (~10%) amorphous organic fine materials and phytoliths present in the groundmass. 10%–20% vertical infillings with well-defined boundaries can be observed, with the original channels filled with fine to medium sand-sized mineral grains such as quartz, feldspar, and pumice (Figure 4A). These coarse grains are similar to the groundmass of upper Layer 6A, suggesting translocation of particles due to pedogenesis processes such as desiccation, root and soil organism activity and cryoturbation (Kooistra and Pulleman, 2018; Kühn et al., 2018). In addition, frequent (30%) sesquioxide hypo-/quasi-coating of voids and infilling areas is present throughout the groundmass (Figure 4), which is formed due to the oxidation and accumulation of Fe/Mn and is most likely caused by rooting (Vepraskas et al., 2018). In summary, Layer 6B has been subjected to various processes of pedogenesis and is probably an old land surface.

3.1.2 Layer 6A

Layer 6A (Samples DD3 and DD4) exhibits a sequence of laminated microfacies of two main alternating types. (1) The lighter laminae ($c/f_{50\mu m}$: 95: 5) exhibit a single grain to pellicular grain microstructure, and consist of well-sorted, fine to medium sand-sized, subrounded to subangular grains, including quartz, feldspar, micas, vitric pyroclast, pyroxene, opaque minerals, etc. (Figure 5A). (2) The darker laminae ($c/f_{50\mu m}$: 90: 10) show a pellicular grain microstructure, and are composed of poorly-sorted, sub-rounded pumices, volcanic glass, and feldspar, ranging in size from 100 to 1000 μm (Figure 5B), which may be the tephra from Tianchi volcano and nearby monogenetic volcanoes (see section 5.1 for a detailed discussion). Reddish-brown silty clay is found coating these coarse tephra, and may be related to the weathering of volcanic glass (Stoops et al., 2018).

Micromorphology sample DD4 contains denser layers of tephra materials, around ten discrete laminae are observed within the 9 cm long sample (Figure 5), suggesting intense and multiple volcanisms in this period. In general, Layer 6A is mainly fluvial sands interrupted with multiple episodes of tephra. No clear evidence of human disruption is observed.

3.1.3 Layers 5 and 4

The Layer 6/5 interface (Sample DD5) is similar in composition to Layer 6 below, but is more disrupted, contains a higher content of fine factions, and shows a pellicular grain to massive microstructure. Shear zones marked by parallel striated clay can be observed in the upper part of the thin section.

Layer 5/4 (Samples DD6, DD7 and DD8) is the mixture of two main fabrics and exhibits a platy to sub-angular blocky microstructure (Figure 6). 1) The "fine" fabric shows a $c/f_{50\mu m}$ of 50: 50. The coarse fraction is composed of poorly sorted, subangular, fine to coarse sand, with occasional (10%) pumices. The fine fraction is composed of dark brown (PPL) fine silty clay with a speckled to grano-striated b-fabric. The voids of this fabric are commonly coated with dusty silty clay. Banded fabrics (Figure 6A), link capping of fine silty clay and dusty silty clay crusts are widely observed, which collectively indicate repetitive freeze-thraw cycles (Van Vliet-Lanoe and Fox, 2018). 2) The 'coarse' fabric is a disrupted version of Layer 6A fluvial sands, but with a few inclusions of pumice. The coarse fractions are commonly coated with dusty silty clay coatings. In Layer 5/4, vertical long cracks later filled with coarse silts and fine sands are observed. In addition, a few (~5%) rounded and irregular-shaped sesquioxide nodules are presented throughout the groundmass, suggesting wet-dry alternations (Vepraskas et al., 2018).

In general, the 'fine' fabric of this layer represents the deposition of low-energy sediments, which is later subjected to land exposure and freeze-thraw disruption. The repeated occurrence of coarser sands is fluvial-derived and suggests a high-energy, unstable depositional environment.

3.1.4 Layer 3

Layer 3 (Samples DD9 and DD10) is similar in composition to the 'fine' fabric of Layer 4 below and presents a granular to sub-angular blocky microstructure with the peds around 1 cm in size. Very dusty, dark brown silty clay complete or partial infilled the complex packing voids between the peds are frequently observed (Figure 7B; Figure 8B). Long cracks later filled with coarse silts and fine sands are also commonly presented. In these infilled areas, sand-size particles are vertically aligned, fine fractions show a striated to strial b-fabric with a high birefringence. Two pieces of obsidian (3–5 mm) with sharp edges are presented, one of which is obliquely aligned in the groundmass (Figure 7A), possibly due to the influence of frost jacking (Van Vliet-Lanoe and Fox, 2018). A few (<5%) rounded, reddish-brown to dark brown sesquioxide nodules are presented throughout the groundmass. In addition, pumices were not observed in the upper part of Layer 4 and the bottom part of Layer 3, but reappeared in the upper part of Layer 3, which may be translocated from the Layer 2 volcanic ashes that are not clearly shown in this profile.

In summary, Layer 3 is composed of relatively stable low-energy sediments later subjected to strong frost actions. The stone artifacts present in this layer show no obvious influence from water actions, but their positions may be altered by the frost jacking process. Translocation of materials from upper layers is frequently observed, which can disturb the original composition and arrangement of particles.

3.1.5 Layer 3/1 interface

The Layer 3/1 interface (Samples DD11) is similar to the Layer 3 below, but with a higher content of coarse fractions, including commonly (20%) present pumices, occasional (15%) rounded sesquioxide nodules, and a few (<3%) root fragments. Round soil peds and relicts of fine silty clay crusts are integrated within the groundmass. This layer could be influenced by both frost action and bioturbation. The high content of pumice may be attributed to pyroclasts from recent Tianchi volcano eruptions.

3.2 Particle size analysis and pH measurement

Layer 7 (JHDD 1) shows the highest sand content (>75%) in the profile, with a Mz of 2.82Φ, which suggest a very high-energy depositional environment (Figure 3). The narrow, single peak (Kg of 1.57) in the frequency distribution curve (Figure 9) indicates a good sorting of particles, presumably suggesting a fine sandy riverbed deposit under high hydrodynamics. Layer 6B (JHDD 2) shows a sudden increase of silt and very fine sand-size particles with a decrease of Mz to 4.77Φ (Figure 3), suggesting a decrease of deposition energy, which is also supported by micromorphological observations that these fine particles constituted the groundmass of the thin section. The wide, multi-peak particle size pattern suggests a more diverse set of sources of the particles (Figure 9), which, based on thin section observation, is caused by the pedogenesis processes that result in the interfusing of coarse grains from upper Layer 6A. The pH of Layers 7 and 6B fluctuated dramatically, which also suggests abrupt changes of the deposition process. Layer 6A (JHDD 3–7) is dominated by medium sand-size and silt-size particles with a Mz of around 3.7Φ, a Kg of around 0.7, and a very negative skewness (Figure 3). Based on micromorphological observations, this layer is composed of well-sorted alluvial sands and tephra coated by fine silty clay. The mixture of these two fabrics may account for the low kurtosis and the double peaks in the frequency distribution curve (Figure 9). The pH in this layer stabilizes at 7.25 to 7.5.

Layer 5/4 (JHDD 8–24) is prevailed by silt-size and clay-size particles with an average Mz of 6.27Φ and shows a wide peak with an input of coarser material in its tail in the frequency distribution curve (Figure 3; Figure 8). These fine materials, based on thin section observation, are fluvially derived low-energy sediments. The fine to medium sands are well-sorted fluvial sands and are more prominent in the upper part of this layer (JHDD 14–24). Layer 3 (JHDD 25–36) shows the finest particle size in the profile, with an average Mz of 7.2Φ. In Layers 3, 4, and 5, the pH gradually decreases to between 6.5 and 7.25. However, sudden decreases in pH value, along with decreases in clay content and increases in sand content in particle size analysis, are observed in samples JHDD 16, 28 and 32 (Figure 3), which may be related to the deposit of volcanic tephra. In Layer 1 (JHDD 37–40), the grain size raises slightly and is dominated by medium silt and a few fine sand. The pH value decreases significantly and the soil becomes more acidic the closer to the ground, which may be related to the accumulation of organic matter in the topsoil (Hong et al., 2019).

4 Discussion

4.1 The site formation process of the Dadong site

Previous studies suggest that the Dadong site shows a transition from blade technology to microblade technology and is dated between 27 and 15 ka, making it an ideal and crucial location to

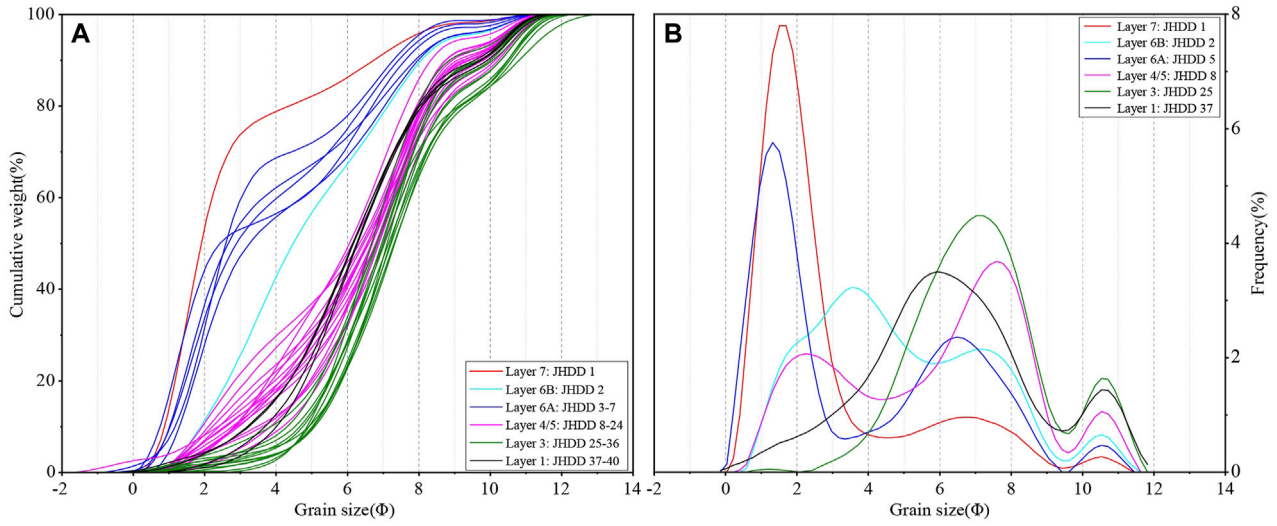

FIGURE 9
Grain size cumulative frequency chart **(A)** and frequency distribution curves **(B)** of the Dadong bulk samples.

examine the emergence and transition of microblade technology (Li, 2008). Using the micromorphological and sedimentological evidence described earlier, this study reconstructs the site formation process at the Dadong site. This will aid in interpreting the dating results, understanding the site's integrity and the significance of the lithic assemblage present.

Above the basal moyite, channel deposits (Layer 7) composed of well-sorted coarse sands and gravel layer are deposited (Figure 2). Pedogenic modification and accumulation of fine materials above the sandy layer (Layer 6B) suggest at least one phase of relative landscape stability around 60-40 ka. In Layer 6A, fluvial sandy deposits reoccurred and are interspersed with multiple episodes of tephra layers. As the dispersion of the pumice and ash fall deposits of the Tianchi volcano is generally towards the East, with volcanic ashes reaching the Japan sea (Figure 1A), it is likely that these tephra layers are the product of explosive eruptions of the Tianchi volcano in Late Pleistocene, probably related to the B-J tephra that is dated to 50.6 ka BP (Okuno et al., 2011; Pan et al., 2020). Eruptions of monogenetic volcanoes may also contribute to the multiple tephra layers observed in Layer 6A. Further geochemical analyses are required to determine the exact source of the tephra layers. In general, the Changbaishan region experienced frequent and intense volcanic activity prior to 50 ka, which could have endangered long-term human occupation and human migration in the region.

In Layers 4/5, alternating fluvial sandy layers and overbank fine-grained sediment are deposited. Associated with the fine-grained sediments are several phases of incipient pedogenesis, implying a relatively stable depositional environment. Therefore, between 25 and 27 ka, this location might have been periodically suitable for human occupation. Layer 3 is dominated by fine-grained alluvial overbank sediment that has undergone strong pedogenesis, representing a phase of landscape stability around 15 ka, making it ideal for human activities.

Besides, no clear tephra layer was detected in Layers 3, 4, and 5. Occasional pumices observed in Layers 4/5 may be transported with other fluvial sands by the Tumen River, suggesting an interval of explosive volcanic activity. This observation also coeval with the hiatus of Tianchi volcanic activities between 50.6 and 8 ka (Pan et al., 2020). Volcanic tephra was detected again in micromorphological samples DD 10 and 11. Combined with the large vertical fissures observed in the thin section and the vertical ice wedges filled with grayish-white sediment observed in the field (Figure 2), these volcanic clasts may be the product of recent volcanic eruptions in the Holocene, which later translocated to the upper part of Layer 3 by strong freeze-thaw action.

Abundant obsidian stone artifacts were unearthed from Layers 3, 4, and 5. However, micromorphological observations show that evidence of repetitive freeze-thaw cycles, such as a typical granular structure, with later infillings of translocated silty clay (Van Vliet-Lanoe and Fox, 2018), can be observed in most of the fine-grained alluvial deposits and are particularly prominent in Layer 3. This may have affected the distribution of lithic artifacts in these layers and caused vertical displacement of the lithics. However, measuring the degree of disturbance is difficult because the rate and extent of lithic translocation are influenced by a variety of factors such as soil moisture, snow/vegetation cover, soil texture, soil permeability, speed of freezing, sediment accretion rate, the size and diameter of the artifact itself, depth of burial, etc. (Johnson and Kenneth, 1974; Hilton, 2003). Further refitting analysis of lithic material and the study of techno-typological consistency may aid in determining the degree and distance of the vertical movement of lithics. In terms of lateral displacement of lithics, movements caused by solifluction are not visible in the Dadong profile because: Layers 3, 4, and 5 are aclinal in a relatively flat floodplain; the artifacts do not show obvious sorting in the upper part of the layer; lateral displacement of lithic artifacts was not observed based on current micromorphology observations. Therefore, the current location of the site can generally reflect site selection and human activities during the middle to late Upper Paleolithic.

In future chronology studies, it should be noted that the translocation of fine particles may cause interference for radiocarbon dating and lithic interpretation. In addition, further residue and micro-wear analyses should take into account the impact of frost action because this process has the potential to transform or remove residues and produce alteration polish on stone artifacts (Michel et al., 2019). Further research is needed to investigate the links between changes in the site formation process, human activity, and the broader environmental and climatic conditions in Northeast China during the Late Pleistocene.

4.2 Environmental change and human adaption in the Changbaishan region

The evolution of the Tumen River terrace and the volcanism of the Changbaishan Volcanoes were the two key factors that influenced Upper Paleolithic human site selection and adaptation at the Dadong site.

Many important Paleolithic sites in China are preserved on river terraces, such as those in the upper reaches of the Hanshui and Danjiang, as well as those on both banks of the You River in the Baise Basin (Pei, 2019). On the one hand, this could be due to the fact that river floodplains with fine-grained overbank deposits are generally low-energy and rarely alter the location of stone artifacts, making them one of the optimum deposit types for conserving the remnants of early human activities (Karkanas and Goldberg, 2018; Pei, 2019). Water, on the other hand, has always been one of the most crucial variables impacting human survival and evolution. In the upper Tumen River, Terraces 1 and 2 are adjacent to the river surface but are quite narrow (Figure 1C), leaving limited space for human activities and occupations. Terraces 3 and 4 on the east bank of the Tumen River and the west bank of the Hongqi River are covered by 80 m-thick Junjianshan Basalt, which was formed during the 2–1 Ma eruptions of the Changbaishan volcanoes (Liu et al., 2015). Although flat and open land is available on top of the Junjianshan Basalt, it is approximately 150 m above the river and has a steep slope (Figure 1C), making it challenging for Paleolithic people to access water and other resources near the river. The floodplain area between the Tumen and Hongqi Rivers is flat, open, and adjacent to the river, making it ideal for human activities (Figure 1C). Micromorphological and sedimentological research of this study reveals that this terrace shows a representative floodplain structure with coarse channel gravels at the base (Layer 7), overlain by horizontal sand layers (Layer 6), and capped by fine overbank silts and clays (Layers 5 to 3). Pedogenic processes were observed in Layers 5 to 3, suggesting a relatively stable deposition environment as well as a dry and exposed land suitable for human activity. These overbank deposits also help to preserve lithic assemblages at Dadong.

At the Dadong site, high-quality and easily accessible obsidians in the beds and banks of the Tumen River may have also been an important consideration during site choosing in the Upper Paleolithic. Although the nature and function of the Dadong site have not been fully defined, manufacturing and processing of stone tools should be one of the key site functions (Wan et al., 2017). Currently, plentiful obsidian stone artifacts, accounting for over 99.9% of the lithic assemblage, have been discovered from the Dadong site, including various tools and abundant by-products of flaking and tool processing, such as flakes and cores (Li, 2008; Zhao, 2012; Wan et al., 2017). Heavy-duty obsidian blade cores weighing 17.4–15 kg are also found at the Xinrenzi Xishan site and the Shirengou site 16 km northwest of the Dadong site (Chen et al., 2006; 2009). Geochemical analysis suggests that the Changbaishan volcanoes are the major geological source of these obsidians in Northeast China and Korea, and the circulation of the obsidian from Changbai volcanoes could reach up to 800 km (Jia et al., 2013; Kuzmin, 2019). An ample supply of obsidian, a raw material particularly suitable for pressure flaking, has made blade reduction a main manufacturing objective of the Paleolithic sites in the Changbaishan region, enabling the application and development of blade and microblade technology in Northeast China (Yue et al., 2021).

As stated previously, Changbaishan volcanic activities have greatly influenced the geomorphology and habitability of the Dadong site. Before 50 ka, this region was generally unsuitable for long-term human occupation due to the frequent eruptions from the Tianchi and nearby monogenetic volcanoes in the Late Pleistocene (Zhang et al., 2018; Pan et al., 2020). The majority of the stone artifacts from this profile were discovered in layers with dates between 27 and 15 ka that are associated with relatively stable sedimentation environments and modest level of volcanic activities, which coincide with the hiatus of the Tianchi volcanism between 50.6 and 8 ka (Pan et al., 2020). In summary, living near active volcanoes can be a two-edged sword. On the one hand, it provides abundant high-quality raw materials, fertile soils, rich plant and animal resources, and a flat landscape suitable for human occupation and migration. On the other hand, destructive volcanic eruptions, such as the B-J and the Millennium Eruption with a VEI≥7 (Pan et al., 2020), could have an impact on the use of the site, the extent of human activity and the adaptation strategy of ancient humans. The example of Dadong demonstrates how Upper Paleolithic people took advantage of natural resources for water, lithic raw materials and probably food supply in a volcanic environment full of risks and hazards, and may shed light on the volcano—human society interactions in the past and present.

5 Conclusion

By using soil micromorphology, particle size analysis, and pH measurements, this study reconstructs the site formation process of the Dadong site from 60 ka to the present. This will aid in the accurate interpretation of lithic assemblages, site integrity, and human behavior of this site, which may also benefit the discussion of the origin and dispersion of microblade technology in northern Eurasia. By reconstructing the development history of the near-bank terrace and the post-depositional process involved, this research may also benefit the study of site formation process and lithic analyses of other important Paleolithic sites in the region. Significantly, as an important pedogenetic agent in this region, the influence of freeze-thawing should be considered in future dating

studies and artifact analyses. Besides, the study of the tephra-rich layer in this profile may also contribute to the understanding of the Late Pleistocene volcanic activity in the southern Changbaishan region. Further tephrochronology studies (Bakker et al., 1996; Economou et al., 2007; Lowe, 2019; Sedov et al., 2011; Stoops et al., 2018) and micromorphological examinations should be conducted to determine the source of the tephra layers, the scale of different eruptions, and to provide reliable stratigraphic chronologies for this region.

Data availability statement

The original contributions presented in the study are included in the article/Supplementary Material, further inquiries can be directed to the corresponding author.

Author contributions

HL designed the research, performed micromorphological analysis and wrote the paper; TX designed the research and directed fieldwork together with WA and YIZ; YUZ and HS performed particle size and pH analyses. KC supervised the research.

Funding

This paper is supported by the major project of "Archaeological China", National Cultural Heritage Administration.

Acknowledgments

We are grateful to the Helong City Museum and the School of Archaeology of Jilin University for their assistance in archaeological excavations. We also thank Junyi Ge for his help and support in the dating. Siqi Li has helped to organize the references.

Conflict of interest

The authors declare that the research was conducted in the absence of any commercial or financial relationships that could be construed as a potential conflict of interest.

Publisher's note

All claims expressed in this article are solely those of the authors and do not necessarily represent those of their affiliated organizations, or those of the publisher, the editors and the reviewers. Any product that may be evaluated in this article, or claim that may be made by its manufacturer, is not guaranteed or endorsed by the publisher.

Supplementary material

The Supplementary Material for this article can be found online at: https://www.frontiersin.org/articles/10.3389/feart.2023.1023773/full#supplementary-material

References

Bakker, L., Lowe, G. J., and Jongmans, A. G. (1996). A micromorphological study of pedogenic processes in an evolutionary soil sequence formed on late Quaternary rhyolitic tephra deposits, North Island, New Zealand. *Quat. Int.* 34–36, 249–261. doi:10.1016/1040-6182(95)00090-9

Boggs, S. (2001). *Principles of sedimentology and stratigraphy*. Upper Saddle River: Prentice-Hall.

Boness, D., and Goren, Y. (2016). Site formation processes at the Late Middle Palaeolithic site of 'ein Qashish: A micromorphological study. *J. Israel Prehist. Soc.* 46, 5–19. Avaliable At: https://www.jstor.org/stable/26572645.

Bullock, P., Fedoroff, N., Jongerius, A., Stoops, G., and Tursina, T. (1985). *Handbook for soil thin section description*. Albrighton: Waine Research Publ.

Catt, J. A. (1985). "Soil particle size distribution and mineralogy as indicators of pedogenic and geomorphic history: examples from the loessical soils of England and Wales," in *Geomorphology and soils*. Editors K. S. Richards, R. R. Arnett, and S. Ellis (London: George Allen and Unwin), 202–218.

Chang, L. Q., Liu, Q. L., Tian, X., Yang, X., and Guo, W. (2018). Analysis on climate characteristics of Helong City, the hometown of longevity in Northeast China. *Mod. Agric. Sci. Technol.* 6, 193+198.

Chen, Q. J., Wang, C. X., Fang, Q., and Zhao, H. L. (2006). Paleolithic artifacts from Shirengou Site, Helong County, Yanbian City. *Acta Anthropol. Sin.* 25 (2), 106–114. doi:10.16359/j.cnki.cn11-1963/q.2006.02.004

Chen, Q. J., and Wang, C. X. (2008). "New findings and studies of Paleolithic Archaeology in Northeast China in recent years," in A Collection of Studies on Archaeology (VII), Festschrift in Commemoration of Professor Lü Zun'e's 80th Birthday and 55 Years of Archaeological Teaching and Research, *comp. School of Archaeology and Museology, Peking University* (Beijing: Science Press), 183–204.

Chen, Q. J., Zhao, H. L., and Wang, C. X. (2009). A report on the excavation at the Xishan Paleolithic Site, Xintunzi County, Fusong City. *Acta Anthropol. Sin.* 28 (2), 147–153. doi:10.16359/j.cnki.cn11-1963/q.2009.02.008

Courty, M. A., Goldberg, P., and Macphail, R. (1989). *Soils and micromorphology in Archaeology*. Cambridge: Cambridge University Press.

Derevianko, A. P., Shimkin, D. B., and Powers, W. R. (1998). *The Paleolithic of Siberia: new discoveries and interpretations*. Urbana and Chicago: University of Illinois Press.

Economou, A., Pateras, D., and Vavoulidou, E. V. (2007). "Volcanic soil resources of Greece," in *Soils of Volcanic Regions in Europe*. Editor Arnalds Ó., Óskarsson H., Bartoli F., and Buurman P. (Berlin; NY: Springer), 25–28. doi:10.1007/978-3-540-48711-1_4

Fan, Q. C., Sui, J. L., Wang, T. H., Li, N., and Sun, Q. (2006). Eruption history and magma evolution of the trachybasalt in the Tianchi volcano, Changbaishan. *Acta Pet. Sin.* 22 (6), 1449–1457.

French, C. (2003). *Geoarchaeology in action: studies in soil micromorphology and landscape evolution*. London: Routledge.

Ge, Y. (2012). Holocene Paleoenvironment reconstruction by using pollen and Phytolith Records in Hanni Peatland. master's thesis. Changchun: Northeast Normal University.

Glauberman, P., Gasparyan, B., Sherriff, J., Wilkinson, K., Li, B., Knul, M., et al. (2020). Barozh 12: Formation processes of a late Middle Paleolithic open-air site in Western Armenia. *Quat. Sci. Rev.* 236, 106276. doi:10.1016/j.quascirev.2020.106276

Goldberg, P., and Macphail, R. I. (2006). *Practical and theoretical Geoarchaeology*. Somerset: Wiley. doi:10.1002/9781118688182

Goldberg, P., Weiner, S., Bar-Yosef, O., Xu, Q., and Liu, J. (2001). Site Formation processes at Zhoukoudian, China. *J. Hum. Evol.* 41 (5), 483–530. doi:10.1006/jhev.2001.0498

Gómez Coutouly, Y. A. (2018). The emergence of pressure knapping microblade technology in Northeast Asia. *Radiocarbon* 60 (3), 821–855. doi:10.1017/RDC.2018.30

Graf, K. E. (2009). "Modern human colonization of the Siberian mammoth steppe: a view from south-central Siberia," in *Sourcebook of Paleolithic transitions*. Editors M. Camps and P. Chauhan (New York: Springer), 479–501. doi:10.1007/978-0-387-76487-0_32

Guo, Y. T. (2021). The discovery and research of the Paleolithic artifacts from the Bu'Erhatong River Basin. master's thesis. Changchun: Jilin University. doi:10.27162/d.cnki.gjlin.2021.003762

Hilton, M. R. (2003). Quantifying postdepositional redistribution of the archaeological record produced by freeze-thaw and other mechanisms: An experimental approach. *J. Archaeol. Method Theory* 10 (3), 165–202. doi:10.1023/A:1026027522255

Hong, S. B., Gan, P., and Chen, A. P. (2019). Environmental controls on soil pH in planted forest and its response to nitrogen deposition. *Environ. Res.* 172, 159–165. doi:10.1016/j.envres.2019.02.020

Jia, L. P., and Huang, W. W. (1984). *Report on the excavation of Zhoukoudian*. Tianjin: Tianjin Science and Technology Press.

Jia, P. W., Doelman, T., Torrence, R., and Glascock, M. D. (2013). New pieces: The acquisition and distribution of volcanic glass sources in Northeast China during the Holocene. *J. Archaeol. Sci.* 40 (2), 971–982. doi:10.1016/j.jas.2012.09.001

Jin, G. Y., and Guo, Z. T. (2011). Soil micromorphology study of the sediment from the Palaeolithic site at Wangfujing, Beijing. *East Asia Archaeol.* 8, 349–352.

Johnson, D. L., and Kenneth, L. H. (1974). The effects of frost-heaving on objects in soils. *Plains Anthropol.* 19 (64), 81–98. doi:10.1080/2052546.1974.11908691

Karkanas, P., and Goldberg, P. (2018). *Reconstructing archaeological sites: understanding the geoarchaeological matrix*. Hoboken, Chichester, West Sussex: Wiley Blackwell.

Kato, S. (2022). Human dispersals and cultural diffusions of Upper Paleolithic in Eastern Eurasia. *Acta Anthropol. Sin.* 41, 12. doi:10.16359/j.1000-3193/AAS.2022.0012

Keates, S. G., Postnov, A. V., and Kuzmin, Y. V. (2019). Towards the origin of microblade technology in Northeastern Asia. *Vestn. St. Petersb. Univ. Hist.* 64 (2), 390–414. doi:10.21638/11701/spbu02.2019.203

Kooistra, M. J., and Pulleman, M. M. (2018). "Features related to faunal activity." chap. 16," in Interpretation of micromorphological Features of Soils and regoliths, *2 nd*. Editors G. Stoops, V. Marcelino, and F. Mees (Amsterdam: Elsevier), 447–469. doi:10.1016/B978-0-444-63522-8.00016-4

Krajcarz, M. T., Kot, M., Pavlenok, K., Fedorowicz, S., Krajcarz, M., Lazarev, S. Yu., et al. (2016). Middle Paleolithic sites of Katta Sai in western Tian Shan Piedmont, Central Asiatic loess zone: Geoarchaeological investigation of the Site formation and the integrity of the lithic assemblages. *Quat. Int.* 399, 136–150. doi:10.1016/j.quaint.2015.07.051

Kühn, P., Aguilar, J., Miedema, R., and Bronnikova, R. (2018). "Textural pedofeatures and related horizons." chap. 14," in Interpretation of micromorphological Features of Soils and regoliths, *2 nd*. Editors G. Stoops, V. Marcelino, and F. Mees (Amsterdam: Elsevier), 377–423. doi:10.1016/B978-0-444-63522-8.00014-0

Kuzmin, Y. V., and Keates, S. G. (2021). Northeast China was not the place for the origin of the Northern Microblade Industry: A comment on. *Paleogeogr. Paleoclimatol. Paleoecol.* 576, 110512. doi:10.1016/j.palaeo.2021.110512

Kuzmin, Y. V. (2019). Obsidian provenance studies in the far eastern and northeastern regions of Russia and exchange networks in the prehistory of Northeast Asia: A review. *Doc. Praeh.* 46, 296–307. doi:10.4312/dp.46.18

Lee, G. K., and Kim, J. C. (2015). Obsidians from the Sinbuk archaeological site in Korea – evidences for strait crossing and long-distance exchange of raw material in Paleolithic Age. *J. Archaeol. Sci. Rep.* 2, 458–466. doi:10.1016/j.jasrep.2015.04.005

Li, H., Zhang, Y. Z., Li, Y. Y., Li, Z. Y., and Jia, Y. N. (2021). Sediment characteristics and the formation processes of Paleolithic sites. [In Chinese]. *Acta Anthropol. Sin.* 40 (3), 363–377. doi:10.16359/j.1000-3193/AAS.2021.0047

Li, W. B., Chen, Q. J., Fang, Q., and Zhao, H. L. (2016). A Preliminary Report on the Trial Excavation at Dadong Paleolithic Site, in Helong, Yanbian, Jilin Province, 2007. [In Chinese]. *Research of China's Frontier Archaeology* 2, 1–11.

Li, X. (2008). A study of the stone artifacts from the Paleolithic Dadong site in Chongshan. master's thesis. Changchun: Jilin University.

Lim, C., Toyoda, K., Ikehara, K., and Peate, D. W. (2013). Late Quaternary tephrostratigraphy of Baegdusan and Ulleung volcanoes using marine sediments in the Japan Sea/East Sea. *Quat. Res.* 80 (1), 76–87. doi:10.1016/j.yqres.2013.04.002

Liu, J. Q., Chen, S. S., Guo, W. F., Sun, C. Q., Zhang, M. L., and Guo, Z. F. (2015). Research advances in the Mt. Changbai volcano. *Bull. Mineralogy, Petrology Geochem.* 34 (4), 710–723. doi:10.3969/j.issn.1007-2802.2015.04.005

Liu, W., Li, Y. Q., and Yang, S. X. (2019). The trial excavation of the Xishantou site of the Paleolithic age in Longjiang County, Heilongjiang Province. [In Chinese]. *Archaeology* 11, 3–13.

Lowe, D. J. (2019). Using soil stratigraphy and tephrochronology to understand the origin, age, and classification of a unique Late Quaternary tephra-derived Ultisol in Aotearoa New Zealand. *Quaternary* 2 (1), 9. doi:10.3390/quat2010009

Macphail, R. I., and Goldberg, P. (2017). *Applied soils and micromorphology in Archaeology*. Cambridge: Cambridge University Press. doi:10.1017/9780511895562

Mallol, C. (2006). What's in a beach? Soil micromorphology of sediments from the Lower Paleolithic site of 'Ubeidiya, Israel. *J. Hum. Evol.* 51 (2), 185–206. doi:10.1016/j.jhevol.2006.03.002

Marder, O., Malinsky-Buller, A., Shahack-Gross, R., Ackermann, O., Ayalon, A., Bar-Matthews, M., et al. (2011). Archaeological horizons and fluvial processes at the Lower Paleolithic open-air site of Revadim (Israel). *J. Hum. Evol.* 60 (4), 508–522. doi:10.1016/j.jhevol.2010.01.007

Michel, M., Cnuts, D., and Rots, V. (2019). Freezing in-sight: the effect of frost cycles on use-wear and residues on flint tools. *Archaeol. Anthropol. Sci.* 11, 5423–5443. doi:10.1007/s12520-019-00881-w

Mingram, J., Stebich, M., Schettler, G., Hu, Y., Rioual, P., Nowaczyk, N., et al. (2018). Millennial-scale East Asian monsoon variability of the last glacial deduced from annually laminated sediments from Lake Sihailongwan, NE China. *Quat. Sci. Rev.* 201, 57–76. doi:10.1016/j.quascirev.2018.09.023

Okuno, M., Torii, M., Yamada, K., Shinozuka, Y., Danhara, T., Gotanda, K., et al. (2011). Widespread tephras in sediments from lake ichi-no-Megata in Northern Japan: Their description, correlation and significance. *Quat. Int.* 246, 270–277. doi:10.1016/j.quaint.2011.08.015

Pan, B., de Silva, S. L., Xu, J. D., Liu, S. J., and Xu, D. (2020). Late Pleistocene to present day eruptive history of the Changbaishan-Tianchi Volcano, China/DPRK: New field, geochronological and chemical constraints. *J. Volcanol. Geotherm. Res.* 399, 106870. doi:10.1016/j.jvolgeores.2020.106870

Patania, I., Goldberg, P., Cohen, D. J., Wu, X. H., Zhang, C., and Bar-Yosef, O. (2019). Micromorphological analysis of the deposits at the early pottery Xianrendong cave site, China: Formation processes and site use in the Late Pleistocene. *Archaeol. Anthropol. Sci.* 11, 4229–4249. doi:10.1007/s12520-019-00788-6

Patania, I., Goldberg, P., Cohen, D. J., Yuan, J. R., Wu, X. H., and Bar-Yosef, O. (2020). Micromorphological and FTIR analysis of the upper Paleolithic early pottery site of Yuchanyan cave, Hunan, South China. *Geoarchaeology* 35 (2), 143–163. doi:10.1002/gea.21771

Pei, S. W. (2019). A general study review of site formation processes for Paleolithic open-air sites. [In Chinese]. *Acta Anthropol. Sin.* 38 (1), 1–18. doi:10.16359/j.cnki.cn11-1963/q.2019.0010

Sedov, S. N., Khokhlova, O. S., and Kuznetsova, A. M. (2011). Polygenesis of volcanic paleosols in Armenia and Mexico: micromorphological records of climate variations in the Quaternary Period. *Eurasian Soil Sci.* 44 (7), 766–780. doi:10.1134/s1064229311070118

Song, Y. H., Cohen, D. J., Shi, J. M., Wu, X. H., Kvavadze, E., Goldberg, P., et al. (2017). Environmental reconstruction and dating of Shizitan 29, Shanxi Province: An early microblade site in North China. *J. Archaeol. Sci.* 79, 19–35. doi:10.1016/j.jas.2017.01.007

Stahlschmidt, M. C., Nir, N., Greenbaum, N., Zilberman, T., Barzilai, O., Ekshtain, R., et al. (2018). Geoarchaeological Investigation of Site formation and depositional environments at the middle Palaeolithic Open-air site of 'Ein Qashish, Israel. *J. Paleolithic Archaeol.* 1 (1), 32–53. doi:10.1007/s41982-018-0005-y

Stebich, M., Mingram, J., Han, J., and Liu, J. (2009). Late Pleistocene spread of (cool-) temperate forests in Northeast China and climate changes synchronous with the North Atlantic Region. *Glob. Planet. Change* 65, 56–70. doi:10.1016/j.gloplacha.2008.10.010

Stoops, G. (2003). *Guidelines for analysis and description of soil and regolith thin sections*. Madison: Soil Science Society of America.

Stoops, G., Sedov, S., and Shoba, S. (2018). "Regoliths and soils on volcanic ash." chap. 25," in Interpretation of micromorphological features of soils and regoliths, *2 nd*. Editors G. Stoops, V. Marcelino, and F. Mees (Amsterdam: Elsevier), 721–751. doi:10.1016/B978-0-444-63522-8.00025-5

Sun, C. Q., Wang, L., Plunkett, G., You, H. T., Zhu, Z. Y., Zhang, L., et al. (2018). Ash from the Changbaishan Qixiangzhan eruption: A new early Holocene marker horizon across East Asia. *J. Geophys. Res. Solid Earth* 123 (8), 6442–6450. doi:10.1029/2018JB015983

Van Vliet-Lanoë, B., and Fox, C. A. (2018). "Frost action." chap. 20," in Interpretation of micromorphological Features of Soils and regoliths, *2 nd*. Editors G. Stoops, V. Marcelino, and F. Mees (Amsterdam: Elsevier), 575–603. doi:10.1016/B978-0-444-63522-8.00020-6

Vepraskas, M. J., Lindbo, D. L., and Stolt, M. H. (2018). "Redoximorphic features." chap. 15," in Interpretation of micromorphological Features of Soils and regoliths, *2 nd*. Editors G. Stoops, V. Marcelino, and F. Mees (Amsterdam: Elsevier), 425–445. doi:10.1016/B978-0-444-63522-8.00015-2

Wan, C. C., Chen, Q. J., Fang, Q., Wang, C. X., Zhao, H. L., and Li, Y. Q. (2017). The discovery, survey and study of the Dadong site in Helong. *Acta Archaeol. Sin.* 1, 1–30.

Wei, H. Q., Liu, G. M., and Gill, J. (2013). Review of eruptive activity at Tianchi volcano, Changbaishan, northeast China: implications for possible future eruptions. *Bull. Volcanol.* 75, 706. doi:10.1007/s00445-013-0706-5

Weiner, S., Xu, Q. Q., Goldberg, P., Liu, J. Y., and Bar-Yosef, O. (1998). Evidence for the use of fire at Zhoukoudian, China. *Science* 281 (5374), 251–253. doi:10.1126/science.281.5374.251

Xu, T., Guo, Y. T., Qiao, X. Y., and Fang, Q. (2021). 2019 report on the Paleolithic archaeological survey of the Bu'Erhatong River Basin (Longjing-Yanji section) in Jilin province. [In Chinese]. *Reg. Cult. Study* 4, 111–119+155.

Yi, M. J., Gao, X., Li, F., and Chen, F. Y. (2016). Rethinking the origin of microblade technology: A chronological and ecological perspective. *Quat. Int.* 400, 130–139. doi:10.1016/j.quaint.2015.07.009

Yue, J. P., Yang, S. X., Li, Y. Q., Storozum, M., Hou, Y. M., Chang, Y., et al. (2021). Human adaptations during MIS 2: Evidence from microblade industries of Northeast China. *Paleogeogr. Paleoclimatol. Paleoecol.* 567, 110286. doi:10.1016/j.palaeo.2021.110286

Zhang, M. L., Guo, Z. F., Liu, J. Q., Liu, G. M., Zhang, L. H., Lei, M., et al. (2018). The intraplate Changbaishan volcanic field (China/North Korea): A review on eruptive history, magma genesis, geodynamic significance, recent dynamics and potential hazards. *Earth-Sci. Rev.* 187, 19–52. doi:10.1016/j.earscirev.2018.07.011

Zhao, H. L. 2012. Experimental research and debitage analysis on the obsidian bifacial point: An example of Dadong Paleolithic Site. dissertation. Helong City, Changchun: Jinlin University.

Zhao, H. L., Xu, T., and Ma, D. D. (2016). Technology and functions of the obsidian burins from the Helong Dadong site in Jilin province. *Acta Anthropol. Sin.* 35 (4), 537–548.